

CAD BASED INTERACTION OF WING STRUCTURES AND AERODYNAMIC LOADS USING FINITE ELEMENT MODEL AND TRANSONIC SMALL DISTURBANCE MODEL

Rais Zain, Indra Nurhadi, Bambang Kismono Hadi, Wayan Tjatra

*Institut Teknologi Bandung
Faculty of Mechanical and Aerospace Engineering
Jalan Ganesha 10, Bandung 40132, Indonesia
tel.: +62 22 2504243, fax: +62 22 2534099
e-mail: rais.fsi@gmail.com*

Abstract

A scheme has been developed to be utilized for solving the interaction between wing aerodynamic loads and the flexibility of wing structures under a quasi static assumption. The interaction is implemented through a link between the nodes of finite element model and the grids of transonic small disturbance model. The particular finite element responses, namely translational displacement vectors (TDV), are utilized for reconstructing the deflected wing surfaces. So in each iteration, the updated surfaces are involved as the parent for regenerating the TSD grids. The criteria of the Euclidean norm is applied for evaluating the convergency of aero-structure interaction. Catia-V5, is fully employed to manage three dimensional geometries for developing the model of wing structures, calculating grids and aerodynamic loads, as well as for reconstructing the updated wing surfaces. Numerous functions and objects of Catia are employed by conducting particular accesses via component object models using Microsoft Visual Basic.Net. A case study is excersized to demonstrate the interaction in transonic speed. The results shown that the scheme is very good in the way performing the interaction in quasi static condition. The utilization of TDV for generating the deflected wing surfaces indicates the capability of high fidelity deformations with respect to the complexity of finite element model.

Keywords: multidisciplinary design, fluid structure interaction, CAD, transonic small disturbance, FEM

1. Introduction

For wings with structural flexibility, the deflection of wings will change the distribution of aerodynamic loads over wing surfaces, then subsequently the loads will alter the deflection of wings. In high subsonic flight the interaction between aerodynamic loads and structure flexibility become more necessary to be considered and solved due to some complexities such as a possibility of shockwave on wing surfaces. Therefore the effect of interaction is appropriate to be addressed in the early stage of wing design in three dimensional models.

Although numerous approaches have been studies, the phenomena of fluid-structure interaction remain challenging. Hou, et al. [4] reviewed several numerical methods, the phenomena broadly classified into two approaches namely the monolithic approach and the partitioned approach. Also it was reviewed several representative of numerical methods based on conforming and non-conforming meshes.

Iqbal et al. [5] utilized Catia-V5 for parametric geometrical input and generate wing model. The wing structures were represented by three dimensional finite element model and ANSYS was utilized to solve the FEM. Matlab was used in conjunction with Microsoft Excel in order to link CFD data with FEM. Another research, Heinrich et al. [2] utilized Catia-V5 for parametric geometry modeling. For aerodynamic loads, it was utilized two versions of solvers governing by the compressible, three-dimensional, time-accurate Reynolds-Averaged Navier-Stokes equations.

Tjatra [10] successfully accomplished a research on transonic aeroelastic of systems with structural nonlinearities. The wing structures were represented by the typical wing section, where

two types of nonlinear springs were selected to represent the structural stiffnesses with respect to pitching and plunging displacements. Aerodynamics loads was computed by Transonic Small Disturbance (TSD) equations with H-type grid distribution. Subsequently Sekar [8], in Munchen University of Technology, contributed some improvements to the aerodynamic model by introducing the scheme of boundary corrections applied for the TSD equations.

Implementing programming on Catia V-5, Zain et al. [11] accomplished an integration from pressure distribution loads to the rigid wingbox model for the purpose of preliminary wing design. In this case the aerodynamics loads was computed by TSD solver developed by Sekar [8]. As presenting in this report, currently the progress comprises the flexibility of wing structures. To perform a validation, it has been investigated the capabilities of the interface between Catia and TSD solver by carrying out the four different wing planforms including RAE 2822 wing [1, 12].

In order to demonstrate the scheme of interaction, a case study was carried out for the wing of small jet airplane applying RAE 2822 airfoils as illustrated in Fig. 1. The side of body becomes a reference for the xz -plane of wing, where its chord line coincides with x -axis and the origin is at its leading edge. The study is carried out at cruising condition about Mach 0.7 and altitude of 35,000 ft.

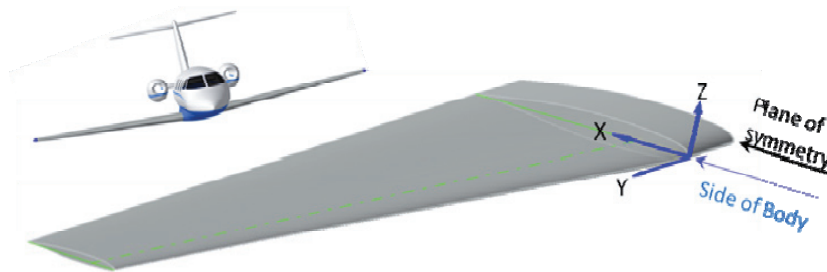


Fig. 1. The spanwise analysis starts at the origin of side of body

2. The scheme of interaction

In the nature of academic necessities, in house software development is commonplace in order to implement ideas and methodologies. As a part of longterm goals to develop the tool for preliminary aircraft design, the scheme of wing design has been developed to be utilized for solving the interaction between wing aerodynamic loads and the flexibility of wing structures under a quasi static assumption operated inside the limit of linear elastic regions. Hopefully the scheme becomes a foundation for further development in order to implement multi-disciplinary optimization.

The solution of aerodynamic loads is run after the responses of wing structures reach a balanced condition. Then the aerodynamic loads act back on the wing structures to produce appropriate responses. For stable wing structures, an iterative sequence will converge to a single condition. In the scheme of this paper, the criteria of Euclidean norm [3] is applied for terminating the iteration. According to the classification proposed by Hou, et al. [4], the scheme is categorized as the partitioned approach with conforming mesh method, i.e. for conforming TSD-grids.

The implementation of the scheme involves thousands of Catia's objects created and linked in specific functionality in order to guarantee that all processes perform consistently and propagate accurately from the highest to the lowest hierarchy. In order to achieve some degree of automation, it is implemented object oriented approaches for utilizing several objects of Catia-V5 in the form of dynamic link library files (DLL) accessed and employed via component object models (COMs). In order to carry out the scheme, several computer programs were created systematically using Microsoft Visual Basic.Net.

The models of wing structures is grouped into *Wing Structural Group* with the primary parent called *Principle Surface* and *Aerodynamic Group* with the primary parent called *Updated Surfaces*. So the updated wing surfaces becomes parent for generating TSD grids and slopes distribution. The distribution of aerodynamic loads is calculated by using the distribution of pressure coefficients

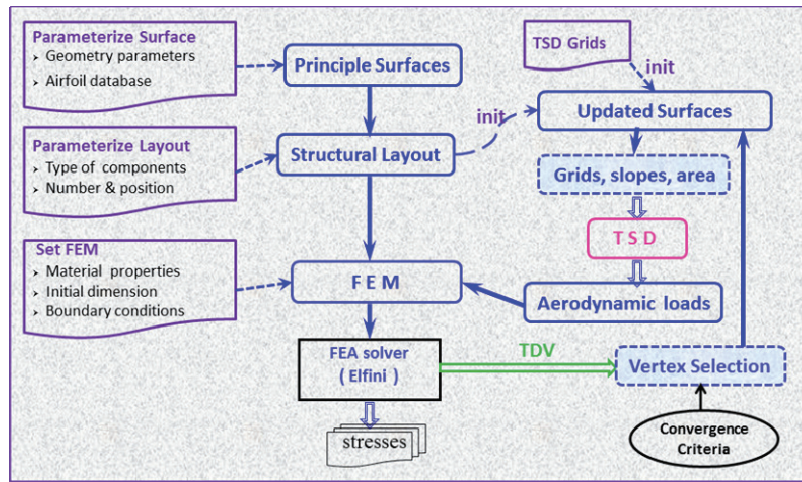


Fig. 2. The scheme of aero-structures interaction

and associated areas and normal vector for each surface panel. In spanwise and chord wise directions, usually the sizes of TSD grids are smaller than the size of FEM grids. So it is required to transform each aerodynamic loads acting on each TSD vertex to the neighborhood nodes of the rib web element by applying the particular transformation provided by Catia.

Structural Layout is utilized to create a layout of wing box structures based on a set of parametric input. The layout is defined by the number of members such as stringers and webs. Then the computer program converts systematically every members into the specific mesh of finite element model, for example a stringer is modeled by 1D-element and a panel of wing skin is modeled by 2D-element [6, 7]. Elfini is applied for finite element analysis to produce several responses such as translational displacement vectors (TDV) and the stresses of elements. In order to reconstruct the deflected wing shapes, it is required to implement the vertex selection for collecting the pertinent vertices of rib nodes.

3. Implementation of the scheme

3.1. Pressure coefficient distribution

The computation of modified TSD involves two types of governing equations namely inviscid in the outer flows and viscous the in inner flows, where the solution of both governing equations can be done by iterative computations [8]. For semi inverse method, at the beginning it is given the initial value of (δ^*_1) for example from flat plate approximation, then the outer inviscid region is solved with direct method to obtain velocity distribution along the surface (U^n_{eOF}), and the inner region is solved by inverse method to get (U^n_{eIF}). It is required to match the two velocity distributions in an iterative module called Relaxation in order to predict the new displacement thickness distribution (δ^*_2) as illustrated in Fig. 3.

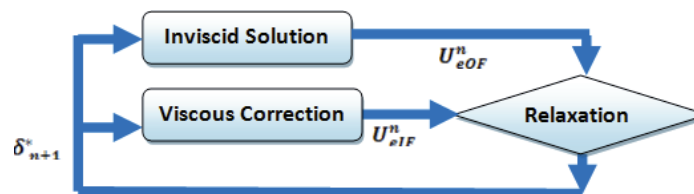


Fig. 3. Illustration of Semi Inverse of displacement thickness

NASA AMES model for transonic small disturbance equation is derived from full potential equation by assuming that all disturbances are small, higher derivative terms are neglected, and the

velocity vector is the same as the gradient of velocity potential. In Cartesian coordinates [8, 10], the continuity equation can be expressed as follows (1) and (2):

$$\frac{\partial f_0}{\partial t} + \frac{\partial f_1}{\partial x} + \frac{\partial f_2}{\partial y} + \frac{\partial f_3}{\partial z} = 0, \tag{1}$$

$$f_0 = -(A\phi_t + B\phi_x), \tag{2a}$$

$$f_1 = E\phi_x + F\phi_x^2 + G\phi_y^2, \tag{2b}$$

$$f_2 = \phi_y + H\phi_x\phi_y, \tag{2c}$$

$$f_3 = \phi_z. \tag{2d}$$

The disturbance velocities ϕ_x , ϕ_y , and ϕ_z are normalized with respect to undisturbed velocity U_∞ . The terms of A, B, E, F, G and H are function of Mach number at free stream and isentropic exponent. In this case the tangential boundary conditions play an important role in TSD, where the slopes of the effective surfaces ϕ_z^\pm [8, 10] are defined by equation (3):

$$\phi_z^\pm = f_x^\pm + \delta_x^\pm. \tag{3}$$

Where δ_x^\pm is the correction of slopes due to the existence of displacement thickness on upper and lower surfaces, and f_x^\pm means the slopes at each vertex of wing surfaces with respect to x -axis. Based on H-type grid distribution [8–10], the distribution of vertices on upper and lower surfaces is created by projecting the grids at planform to the surfaces by the application on Catia as shown in Fig. 4. Then in Fig. 5 it is depicted the distribution of C_p at Section-15 for upper and lower surfaces, along with η is the ratio of grids location in y -direction over semi span.

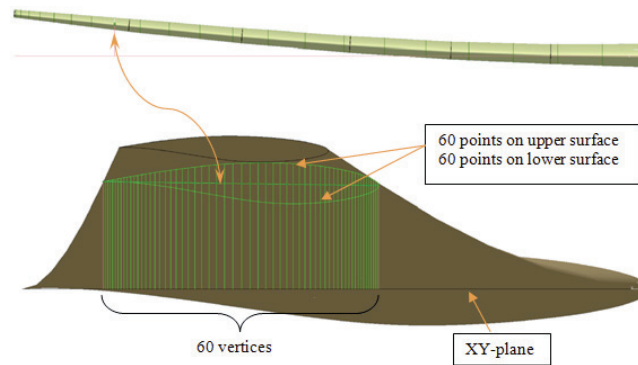


Fig. 4. The projection of grids at the planform of upper and lower surfaces at Section 15 or $\eta = 0.841$

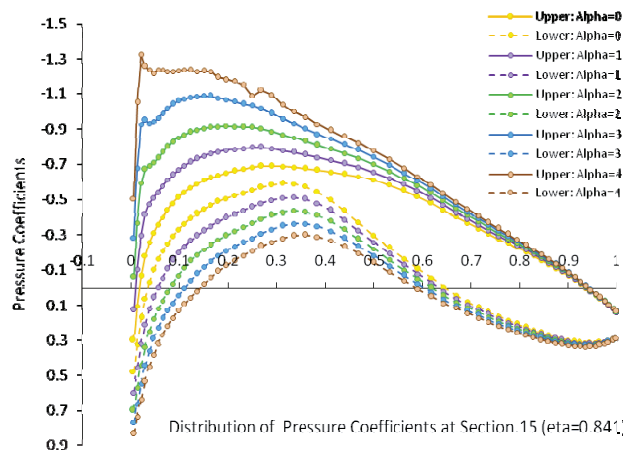


Fig. 5. The comparison of C_p due to variation of angle of attack at Section 15

3.2. Wing structure model

In order to reconstruct a deflected wing shape, a standard wing box model is not sufficient due to unavailability information concerning with the translation displacement of rib vertices from leading to front spar and from rear spar to trailing edge, which is very essential for reconstructing all wing sections. Therefore it is proposed to apply a complete series of rib web model, so each rib web is fully modelled from leading edge to trailing edge as shown in Fig. 4.

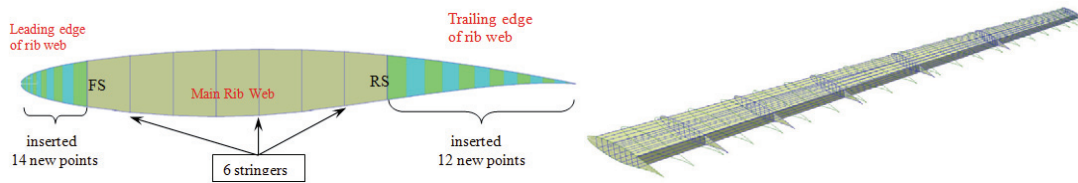


Fig. 4. The wing-box model with leading edge and trailing edge rib webs

3.3. Matching TSD grids and the structural layout

To achieve higher distribution toward wing tip direction, a number of TSD grids are inserted to each rib spacing to keep them intact with the parent. Fig. 5 depicts a zooming portion and shows that the distribution of TSD Grids is arranged almost cosine in spanwise direction.

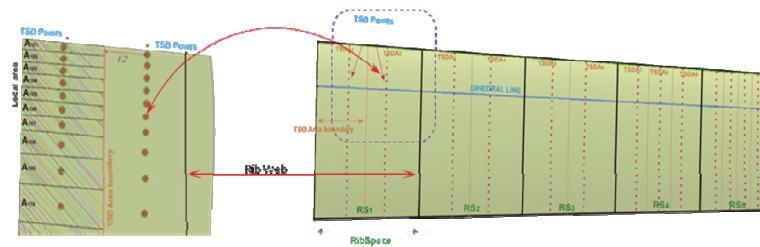


Fig. 5. The distribution of TSD grids and panel area between rib spacing

The transformation of each normal force from the centroid of rectangle panel to the four nodes of 2D-element utilizes the functions of Catia. Fig. 5 shows the distribution of normal forces on the upper and lower surfaces.

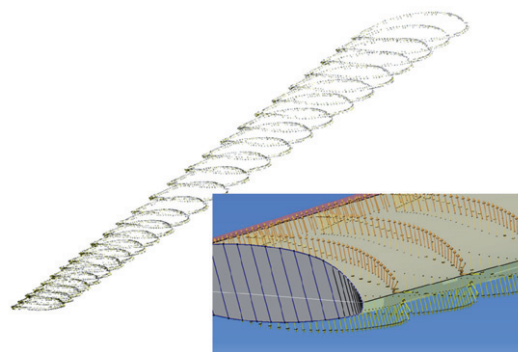


Fig. 6. The distribution of normal forces in chordwise and spanwise

3.4. Convergence criteria

An iterative solution is implemented to determine whenever the current run is close enough to fulfill the termination criteria of Euclidean norm criteria (4). The iteration will be stopped if the ratio of (n) -iteration over the $(n-1)$ -iteration of Euclidean norm is less than 1%.

$$\frac{\left\{ \left[\sum_{j=1}^m \sum_{i=1}^3 (v_i)^2 \right]^{0.5} \right\}_{(n)}}{\left\{ \left[\sum_{k=1}^m \sum_{j=1}^3 (v_i)^2 \right]^{0.5} \right\}_{(n-1)}} \leq \varepsilon, \tag{4}$$

where:

- ε – the termination criteria is proposed to be $\varepsilon < 1\%$,
- v – variable of translational displacement vector, $TDV = V = [v_x, v_j, v_z]$,
- i – iteration control for degree of freedom direction, in this case are (x, y, z) directions,
- j – iteration control for number of vertices,
- m – number of vertices,
- n – number of iteration.

4. Generating consecutive surfaces

The result of *Vertex Selection* is a set of proper TDV for reconstructing the current rib shapes. Then the splines of updated ribs can be used for creating the deflected wing surfaces by using multi-sectional technique. In Fig. 7 the red surfaces are generated in the first time (before applying loads) by using information from initial structural layout, then the brown surfaces are the result of the second updated surfaces.

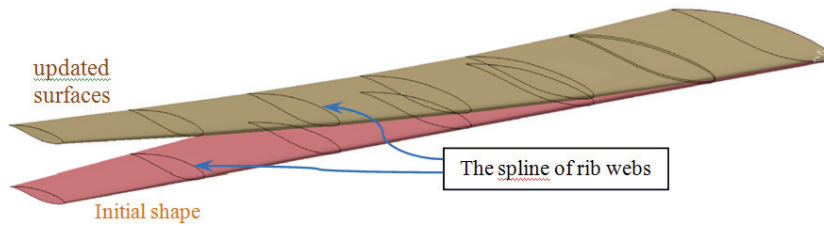


Fig. 7. The distribution of normal forces in chordwise and spanwise

To show the step of updated wing surfaces, it is carried out five consecutive run as summarized in Tab. 1. Also it is visualized in series the result of Run_1 until Run_5 in global coordinate system.

Tab. 1. The sequence of Run_# involving iterative TDV and Update Surfaces

<p>Run_1 : Updated Surface_1 is generated from Structural layout (initialization)</p> <p style="padding-left: 20px;">Update: TSD model, and aerodynamic forces</p> <p style="padding-left: 20px;">Result in: TDV_1</p>
<p>Run_2 : Updated Surface_2 is generated from TDV of Run_1</p> <p style="padding-left: 20px;">Update: TSD model, and aerodynamic forces</p> <p style="padding-left: 20px;">Result in: TDV_2</p>
<p>.....</p>
<p>Run_n : Updated Surface_n is generated from TDV of Run_(n-1)</p> <p style="padding-left: 20px;">Update: TSD model, and aerodynamic forces</p> <p style="padding-left: 20px;">Result in: TDV_n</p>

The following pictures are the results of consecutive regenerating surfaces namely Run_1 is pink, Run_2 is brown, and Run_3 is green, Run_4 is blue, and Run_5 is yellow as depicted in Fig. 8.

In order to make them easier to compare, several pictures are depicted together in series of Run_# as shown in Fig. 9.

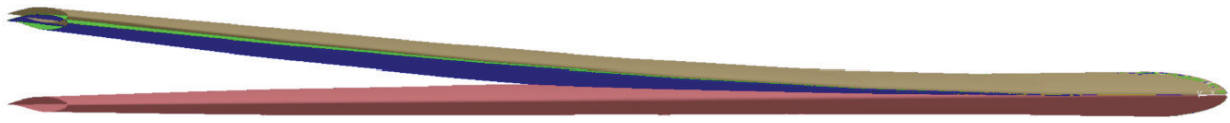


Fig. 8. Visualization of consecutive wing surfaces from Run_1 to Run_5

In order to show it more clearly, deflections of the tip-end sequentially resulted in Run_1 to Run_5 depicted in Fig. 9. It can be seen that the ribs of Run_2 move upward such that the plane of some ribs are no longer parallel to the original xz -plane. As TSD grids are attached relatively to FEM, they move together with the FEM of Run_2. Eventhough the ribs move upward such that, all the projection of TSD grids to surfaces are still parallel to the xz -plane.

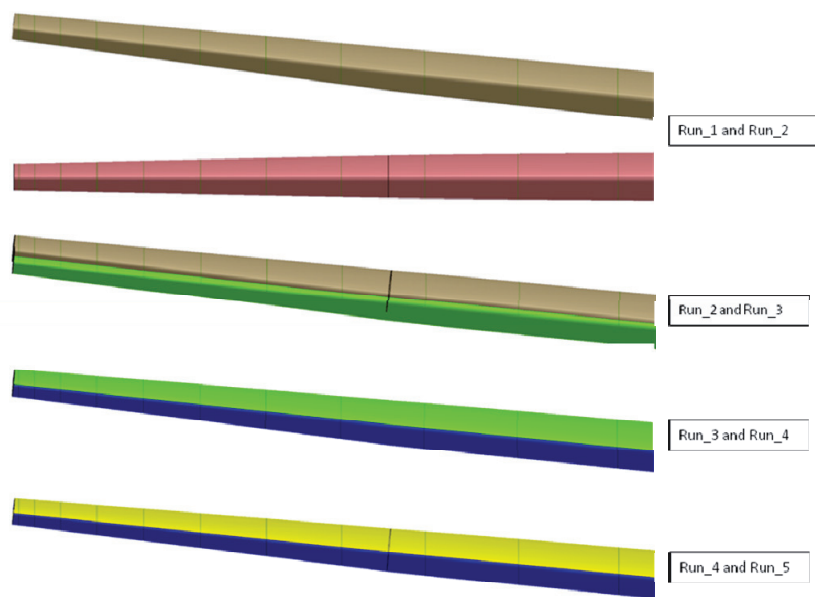


Fig. 9. Visualization of sequence consecutive wing surfaces at tip end

The series of visualization in Fig. 9 illustrates that the deflections of Run_3, Run_4, and Run_5 are in balance condition indicated by small alteration. Finally the termination criteria expressed in (4) is executed, where the result is presented in Tab. 2. It is found that Run_3 already fulfilled the convergence criteria of Euclidean norm by value of 0.72%.

Tab. 2. Termination criteria by Euclidean norm

Run#	Eucl Norm	Criteria (%)
1	2441.9	
2	182.4	7.47
3	17.5	0.72
4	15.5	0.63
5	2.1	0.09

5. Conclusion

- (a) Based on the sequence of iteration as shown in Section-4, the use of Euclidean norm criteria expressed in Equation (4) enable one to solve the scheme of interaction between aerodynamic loads with the flexibility of wing structures within linear elastic regions. Both, visuallization

shown in Fig. 9 and calculation of Euclidean norm criteria depicted in Tab. 2 verify that the deflected wing surfaces converge to a particular condition.

- (b) Using termination criteria (4), it is found that Run_3 already fulfilled the convergence criteria of Euclidean norm by value of 0.72%. Also the values of ε become smaller from Run_3 to Run_5, these values mean that alterations are consistently reduced for consecutive Run_#.
- (c) The application of a wing box with full rib webs model applied for the finite element analysis is appropriate to provide a set of complete data for translational displacement vectors from leading edge to trailing edge.
- (d) The use of *Updated Surfaces* for calculating the slopes and the grids to become a set of input for TSD solver indicates very good results in terms of accuracy. Also the technique of accessing Catia's objects can be applied as well for calculating the normal vectors and the area of panels which are required for calculating normal forces.

Acknowledgment

This research has been made possible by the partial funding from "Lembaga Penelitian dan Pengabdian kepada Masyarakat" (Institute for Research and Community Services), *Institut Teknologi Bandung*, under the research contract No. 2292/I1.B04/KU/2103.

References

- [1] Cook, P. H., McDonald, M. A., Firmin, M. C. P., *Aerofoil RAE 2822 Pressure Distributions; Boundary Layer and Wake Measurements*, AGARD AR-138 Experimental Data Base for Computer Program Assessment, Royal Aircraft Establishment, United Kingdom 1979.
- [2] Heinrich, R., Kroll, N., Neumann, J., Nagel, B., *Fluid-Structure Coupling for Aerodynamic Analysis and Design – A DLR Perspective*, AIAA 2008-561, 46th AIAA Aerospace Sciences Meeting and Exhibit, Reno, Nevada, United States 2008.
- [3] Hinton, E., *NAFEMS Introduction to Nonlinear Finite Element Analysis*, NAFEMS Birniehill East Kilbrige, Glasgow, UK 1992.
- [4] Hou, G., Wang, J., Layton, A., *Numerical Methods for Fluid-Structure Interaction – A Review*, Commun. Comput. Phys., Vol. 12, pp. 337-377, 2012.
- [5] Iqbal, L. U., Sullivan, J. P., *Application of an Integrated Approach to the UAV Conceptual Design*, AIAA 2008-144, 46th AIAA Aerospace Sciences Meeting and Exhibit, Reno, Nevada, United States 2008.
- [6] Niu, M. C. Y., *Airframe Structural Design*, Conmilit Press Ltd., Hong Kong 1988.
- [7] Niu, M. C. Y., *Airframe Stress Analysis and Sizing*, Conmilit Press Ltd., Hong Kong 1988.
- [8] Sekar, W. K., *Viscous-Inviscid Interaction Methods for Flutter Calculations*, Dissertation in University of Munchen, Germany 2006.
- [9] Thompson, J. F., et al., *Numerical Grid Generation; Foundations and Applications*, Elsevier Science Publishing Co., Amsterdam, The Netherlands 1985.
- [10] Tjatra, W., Kapanla, R. K., *Transonic Aeroelastic of Systems With Structural Nonlinearities*, VPI, Virginia 1991.
- [11] Zain, R., Nurhadi, I., Hadi, B. K., Tjatra, W., *CAD Based Integration from Pressure Distribution Loads to Wingbox Model for Preliminary Wing Design*, Regional Conference on Mechanical and Aerospace Technology, Bangkok 2013.
- [12] Zain, R., Atmadi, S., Fitroh, A. J., *Development and Validation for the Interface between Catia – TSD Solver*, Regional Conference of Siptekgan, LAPAN, Jakarta 2013.